A Method to Determine Stress-Dependent Filtration Properties of Fractured Porous Rocks by Laboratory Test Data

Larisa Nazarova[1,*], *Leonid* Nazarov[1] , *Nikita* Golikov[2] and *Alexandr* Skulkin[1]

[1]Chinakal Institute of Mining, Siberian Branch, Russian Academy of Sciences, 630091, Novosibirsk, Russia
[2]Trofimuk Institute of Petroleum Geology and Geophysics, Siberian Branch, Russian Academy of Sciences, 630090, Novosibirsk, Russia

Abstract. Within the dual porosity model the authors develop and theoretically, using synthetic data, substantiate the method for determining mass exchange coefficient and stress-dependent permeability of fractured porous reservoir rocks. The proposed filtration test circuit consists of three sequential measurements of flowrate in a specimen subjected to the varied external stress σ at the inlet fluid pressure P: by standard scheme (Q_0) and with plugging of fissures at one (Q_1) and at the other end (Q_2) of the specimen. The model of the experiment is created, and the analytical solution is obtained for the direct problem on steady-state flow: dependences of Q_0, Q_1 and Q_2 on σ and P. The input data are synthesized by superimposition of multiplicative noise on the exact solution of the direct problem. The synthesized data are used to derive the inversion relations for calculating the permeabilities k_1 and k_2 of fissures and matrix as well as the mass exchange coefficient by Q_0, Q_1 and Q_2. Using LS method, the dependences $k_1(\sigma)$ and $k_2(\sigma)$ are reconstructed. The numerical experiments reveal low stability of inversion by input data. Thus, it is necessary to perform a cycle of measurements at the increasing input pressure with subsequent averaging of the results.

1 Introduction

Justification of opening and mining schemes in hydrocarbon extraction, estimation of well stability, inversion of logging data - this is a far from being complete list of problems solvable using knowledge on poroperm properties of reservoir rocks [1-3]. The source of such information can be laboratory experiments, field tests and integrated geophysical logging [4, 5]. The obtained data are interpreted in the framework of hydrodynamic models usually selected based on the petrographic analysis of core samples [6].

---

*Corresponding author: <u>lanazarova@ngs.ru</u>

Productive strata in many hydrocarbon reservoirs have porous and fractured structure [7]. For description of fluid flow in such strata, in [8] a dual porosity model is proposed for a medium composed of elements of two types - matrix and fissures (Fig. 1). Each type is provided with a set of the governing parameters (pressure, permeability, porosity, etc.) and the law of mass exchange between the constituent elements. Later on, this approach was generalized to any types of continuum [9-11] by introduction of notion of a *representative elementary volume* and was successfully applied in studying heat and mass transfer processes in multi-phase systems [12, 13], including oil and gas reservoirs [14-17] and coal rock masses [18-22].
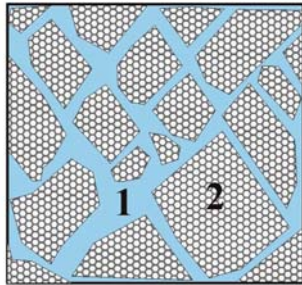

Fig. 1. Structure of fractured porous medium: 1 – fissures; 2 – matrix.

One of the stages in verification of such models is estimation of permeability and porosity of constituent elements, as well as determination of an empirical function *M* describing mass exchange between matrix and fissures. The objective is reached using data of laboratory [23, 24] and full-scale [25-27] tests, as well as calculated effective parameters of media with regular [28, 29] and stochastic [30, 31] structure. In [8, 25], it is assumed that the function *M* can only be determined in the transient mode of well operation using the pressure build-up curve.

The laboratory [32-36] and in-situ [37-39] researches prove the essential dependence of rock permeability on stresses. With increasing depth, this effect exerts stronger influence on efficiency of geophysical log data interpretation aimed to identify producing intervals and estimate poroperm properties of reservoir rocks [40, 41].

This paper, within the model of the fractured porous medium [8], develops and theoretically substantiates the method which makes it possible to determine the empirical function of mass exchange between matrix and fissures as well as the dependence of their permeabilities on stresses by the data of stationary filtration tests.

2 Model of Fractured Porous Medium

Evolution of hydrodynamic fields in a fractured porous medium is described with the dual porosity model [8] including:
the continuity equations
$$(\varphi_1\rho_1)_{,t} + \nabla\cdot(\rho_1\mathbf{V}_1) + M = 0, \qquad (\varphi_2\rho_2)_{,t} + \nabla\cdot(\rho_2\mathbf{V}_2) - M = 0; \qquad (1)$$
Darcy's law
$$\mathbf{V}_m = -k_m\nabla p_m/\eta, \qquad (2)$$
and the state equations
$$\rho_m/\rho_0 = 1 + c(p_m - P_a), \qquad \varphi_m = \varphi_m^0 + c_m(p_m - P_a), \qquad (3)$$
where subscripts 1 and 2 denote values related with fissures and matrix, respectively, and superscript 0 - values of the same parameters under the atmospheric pressure P_a; $\mathbf{V}_m$ is the

fluid flow velocity ($m = 1,2$); ρ_m, φ_m and c_m are the density, porosity and compressibility of solid substance; ρ, η and c are, respectively, the density, viscosity and compressibility of fluid. The laboratory tests [34, 35, 42, 43] show that under low pressures, the permeability dependence on stresses is well approximated by the exponential function

$$k_m = K_m \exp(-\alpha_m \sigma), \tag{4}$$

K_m and α_m are empirical constants. In case of comparable pressure and stresses, σ in (4) should be interpreted as an effective stress $\sigma - p_m$. For rocks with porosity of 5-20%, $\alpha_2 \cong 0.001$-0.1 MPa^{-1}.

In [8, 43] it is proposed to describe intensity of crossflows between matrix and fissures by the linear function

$$M(p_1, p_2) = \rho_0 \beta (p_2 - p_1)/\eta, \tag{5}$$

where β is the mass exchange coefficient. In [8, 25] it is mentioned that β depends on the specific surface of matrix rocks.

When fluid, matrix and fissures are the weakly compressible media, system (1)-(3) can be linearized and, with regard to (5), reduced to two equations

$$
\begin{aligned}
(c_1 + c\varphi_1^0)\eta \frac{\partial p_1}{\partial t} &= k_1 \Delta p_1 - \beta (p_2 - p_1), \\
(c_2 + c\varphi_2^0)\eta \frac{\partial p_2}{\partial t} &= k_2 \Delta p_2 + \beta (p_2 - p_1).
\end{aligned}
\tag{6}
$$

3 Formulation and Solution of Boundary Problem

Let a cylindrical specimen (base area S, length l) be subjected to a constant stress σ over lateral surface (Fig. 2). We consider a one-dimensional steady-state flow described by the system of equations obtained from (6)

$$
\begin{aligned}
k_1 \frac{\partial^2 p_1}{\partial x^2} - \beta (p_2 - p_1) &= 0, \\
k_2 \frac{\partial^2 p_2}{\partial x^2} + \beta (p_2 - p_1) &= 0,
\end{aligned}
\tag{7}
$$

where p_1 and p_2 are the functions of the coordinate x directed along the specimen axis. The permeability-stress dependence is included in (7) through (4).
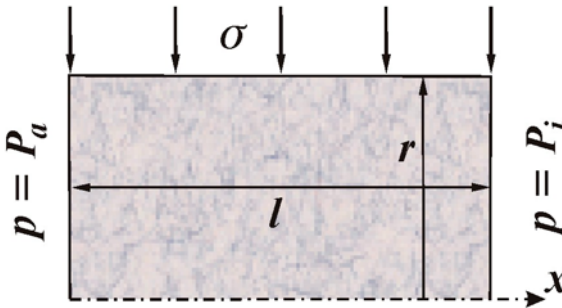

Fig. 2. Scheme of experiment.

As per the study objective, it is required to develop the filtration test pattern such that to find the mass exchange coefficient and constants in empirical dependences (4) of stress-

dependent permeabilities of matrix and fissures. Determination of the parameters k_1, k_2 and β included in (7) needs not less than three 'quantums' of information obtained on the same specimen. The three sequential measurement designs are presented below with relevant boundary conditions for (7).

T0. Standard filtration tests [45]

$$p_1(0) = p_2(0) = P_a , \qquad p_1(l) = p_2(l) = P_i ,$$

P_i is the inlet pressure (Fig. 2).

T1. On the left end, fissures are plugged with a penetrant, and using a high resolution image (obtained, e.g., with electron microscope), the area S_1 of these fissures is determined. On the right end $x = l$, the fluid pressure P_i is set; on the left end, the atmospheric pressure is assigned

$$V_1(0) = 0 , \quad p_2(0) = P_a , \qquad p_1(l) = p_2(l) = P_i .$$

T2. The right end fissures are plugged and then

$$V_1(0) = 0 , \quad p_2(0) = P_a , \qquad V_1(l) = 0 , \quad p_2(l) = P_i .$$

In all tests T0, T1 and T2, the fluid flow rates Q_0, Q_1 and Q_2 are measured on the left end in the steady-state flow mode.

Omitting cumbersome intermediate calculations, Table 1 presents the final result, namely, the pressure distribution in matrix and fissures, as well as the fluid flowrate at $x = 0$.

Table 1. Solving system of equations (7) at the boundary conditions T0, T1 and T2

T0	$p_1(\xi) = p_2(x) = P_a + (P_i - P_a)\xi$ (8)
	$Q_0 = \dfrac{k_1(\delta + \psi)(p_c - p_a)S}{(1+\delta)l\eta}$ (9)
T1	$p_1(\xi) = P_a + (P_i - P_a)\dfrac{D(\gamma,\xi) + \xi\sin\gamma(1-\xi)}{D(\gamma,1)}$ $p_2(\xi) = P_a + (P_i - P_a)\dfrac{D(\gamma,\xi) - \sin\gamma(1-\xi)}{D(\gamma,1)}$ (10)
	$Q_1 = \dfrac{\psi k_1(p_c - p_a)S}{(1+\delta)l\eta}G(\gamma,\xi)$ (11)
T2	$p_1(\xi) = P_a + (P_i - P_a)\dfrac{D(\gamma,\xi) + \xi\sin\gamma(1-\xi)}{D(\gamma,1)}$ $p_2(\xi) = P_a + (P_i - P_a)\dfrac{D(\gamma,\xi) - \sin\gamma(1-\xi)}{D(\gamma,1)}$ (12)
	$Q_2 = \dfrac{\psi k_1(p_c - p_a)S}{(1+\delta)l\eta}G(\gamma/2,\xi)$ (13)

In (8)-(13) we introduced symbols $\xi = x/l$, $\psi = k_2/k_1$, $\gamma = l\sqrt{\beta(1+\psi)/k_1}$, $\delta = S_1/(S - S_1)$, $D(\gamma,\xi) = \sin\gamma + \gamma\psi\xi\cos\gamma$, $G(\gamma,\xi) = \gamma(1+\psi)/(\tan\gamma + \psi\gamma)$.

Figure 3a depicts the pressure in matrix in the test design T2 at $P_i = 0.2$ MPa, $P_a = 0.1$ MPa, $\psi = 0.02$ and different values of γ. The distribution of p_2 is asymmetrical relative to the middle of the specimen.

Figure 3b demonstrates the contour lines of the dimensionless flowrate $G(\gamma,\psi)$: G weakly depends on γ at small ψ. This is one of the reasons for instable inversion of the experimental results by the input data (paragraph 4).
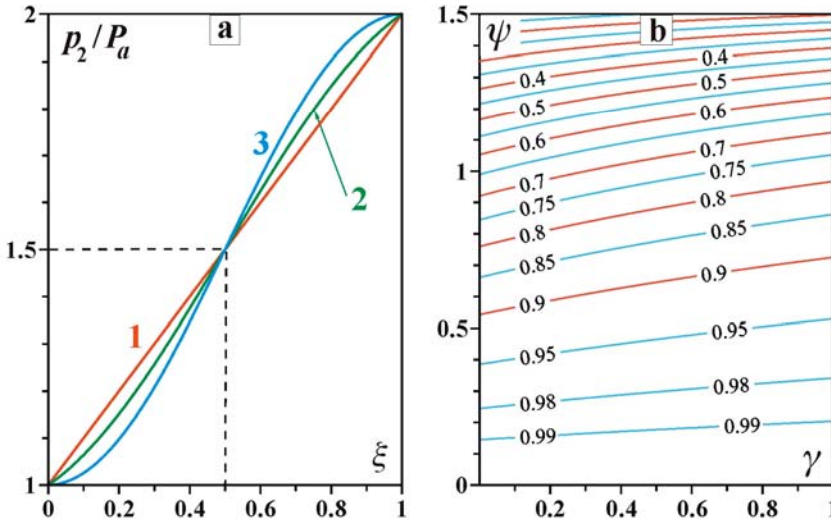
Fig. 3. Pressure distribution in matrix at boundary conditions T2 (a); contour lines of function G (b).

4 Inversion of Experimental Results

4.1 Synthesis of Input Data

We set some values for the permeabilities $K_1 = K_1^*$ and $K_2 = K_2^*$, mass exchange coefficient $\beta = \beta^*$, as well as the parameters $\alpha_1 = \alpha_1^*$ and $\alpha_2 = \alpha_2^*$. The specimen has radius $r = 0.2$ cm ($S = 12.57$ cm^2) and length $l = 8$ cm; the relative area of fissures on the left end is $\delta = 0.001$, the fluid viscosity is $\eta = 10^{-5}$ Pa·s (air). For each value of the inlet pressure P_i and external stress $\sigma = \sigma_n$ in the chosen ranges $[P_{\min}, P_{\max}]$ and $[\sigma_{\min}, \sigma_{\max}]$, from formulas (9), (11) and (13), we calculate the flow rates $Q_s^*(i,n)$ ($s = 0,1,2$) and synthesize input data by superposing the exact values with multiplicative noise

$$Q_s(i,n) = [1 + \omega_s(i,n)]Q_s^*(i,n) , \qquad (14)$$

where $\omega_s(i,n)$ are random values uniformly distributed in the segment $[-\varepsilon, \varepsilon]$, ε is a relative error of measurements. Modern flowrate meters have ε lesser than 0.5-1% [46].

The numerical experiments involved $K_1^* = 2500$ mD, $K_2^* = 125$ mD, $\beta^* = 0.012$, $\alpha_1^* = 0.025$ MPa^{-1}, $\alpha_2^* = 0.005$ MPa^{-1}, $P_{\min} = 0.2$ MPa, $P_{\max} = 0.7$ MPa, $\sigma_{\min} = 0$, $\sigma_{\max} = 5$ MPa. Table 2 presents the input data (columns 2, 3 and 4) generated using (14) at $\varepsilon = 0.01$.

4.2 Determination of Poroperm Parameters of Fractured Porous Medium

Denote $u_1 = Q_1(i,n)/Q_0(i,n)$, $u_2 = Q_2(i,n)/Q_0(i,n)$, then, dividing (11) and (13) by (9), we obtain

$$\psi G(\gamma, \psi)/(\delta + \psi) = u_1 , \qquad \psi G(\gamma/2, \psi)/(\delta + \psi) = u_2 . \qquad (15)$$

The Macluarin expansion of the tangent at small γ reduces (15) to a system of equations with respect to γ and ψ

$$\frac{\psi(1+\psi)}{(\delta+\psi)(1+\psi+\gamma^2/3)} = u_1, \qquad \frac{\psi(1+\psi)}{(\delta+\psi)(1+\psi+\gamma^2/12)} = u_2 \qquad (16)$$

which has an analytical solution (columns 5 and 6, Table 2)

$$\psi = \frac{3u_1u_2\delta}{4u_1-u_2-3u_1u_2}, \qquad \gamma^2 = \frac{12(1+\psi)(u_2-u_1)}{4u_1-u_2} \qquad (17)$$

The permeability of fissures at the preset external stress σ_n and inlet pressure P_i is found from (9)

$$k_1 = \frac{\eta l(1+\delta)Q_0(i,n)}{(P_i-P_a)(\delta+\psi)S}$$

(columns 6), the matrix permeability $k_2 = \psi k_1$ (columns 8) and, finally, the mass exchange coefficient

$$\beta = \frac{\gamma^2 k_1}{\eta l^2(1+\psi)}$$

(columns 10). For each σ_n, from (4) we find the exact values of the permeabilities $k_m^* = K_m^* \exp(-\alpha_m^* \sigma_n)$ and calculate the relative errors $\lambda_1 = |1-k_1/k_1^*|$ and $\lambda_2 = |1-k_2/k_2^*|$, as well as $\lambda_\beta = |1-\beta/\beta^*|$ (columns 8, 10 and 12, Table 2). It turns out that even at the small measurement error of the flowrate, the determination error of k_1 and β can exceed 70%. The cause of such errors lies in the contrast of the permeabilities of matrix and fissures as they can differ by 1-3 orders of magnitude [25]. For better accuracy, it is necessary to measure flow rates at several values of the input pressure P_i and to assume the required values as average quantities (last line in Table 2).

Table 2. Input data generated at $\sigma = 3$ MPa and the virtual experimental results.

1	2	3	4	5	6	7	8	9	10	11	12
P_i MPa	Q_0 l/min	Q_1 l/min	Q_2 l/min	ξ	γ	k_1 mD	λ_1, %	k_2 mD	λ_2, %	β	λ_β, %
0.20	1.03	0.99	1.01	0.1140	0.3177	946.8	19.8	107.9	0.3	1.528	27.3
0.25	1.55	1.48	1.51	0.1016	0.3026	1060.2	10.2	107.8	0.2	1.399	16.6
0.30	2.05	1.98	2.01	0.0977	0.2605	1102.1	6.7	107.7	0.1	1.040	13.3
0.35	2.57	2.48	2.52	0.1155	0.2830	934.3	20.9	107.9	0.3	1.211	0.9
0.40	3.09	2.97	3.03	0.1247	0.3067	866.5	26.6	108.0	0.4	1.412	17.6
0.45	3.59	3.45	3.52	0.1382	0.3215	782.4	33.7	108.1	0.5	1.535	27.9
0.50	4.09	3.95	4.04	0.2254	0.3326	481.7	59.2	108.6	0.9	1.531	27.6
0.55	4.65	4.44	4.52	0.0627	0.2736	1704.5	44.3	106.9	0.7	1.176	2.0
0.60	5.13	4.93	5.04	0.1443	0.3254	749.5	36.5	108.2	0.6	1.564	30.3
0.65	5.67	5.42	5.52	0.0642	0.2691	1664.7	41.0	106.9	0.6	1.137	5.3
0.70	6.18	5.95	6.06	0.1096	0.2874	983.9	16.7	107.9	0.3	1.255	4.6
						1025.1	13.2	107.8	0.2	1.344	12.0

4.3 Determination of Stress-Dependent Permeabilities of Matrix and Fissures

For the model parameters accepted in 4.2 but at $\varepsilon = 0.02$, using (14), we synthesize input data for P_i=0.2, 0.25,…,0.7 MPa and σ_n=0, 1,…,5 MPa, perform inversion and find permeabilities for fissures, $k_1(i,n)$, and matrix, $k_2(i,n)$ (columns 2-7, Tables 3 and 4).

Table 3. Virtual experimental results on reconstruction of the dependence between the fissure permeability k_1 and stresses.

1	2	3	4	5	6	7	8	9	10	11	12
P_i MPa	σ_n, MPa						K_1 mD	θ_1 %	α_1 MPa^{-1}	θ_α %	ν_{1i} %
	0	**1**	**2**	**3**	**4**	**5**					
0.20	2506.6	1979.1	1226.6	904.9	1418.9	494.0	2455.1	1.8	0.02692	7.7	19.3
0.25	2308.0	2049.5	1258.3	1065.1	1264.2	1026.1	2130.0	14.8	0.01620	35.2	13.8
0.30	2929.4	1820.7	2092.1	1442.3	382.7	930.6	2890.2	15.6	0.03081	23.3	22.4
0.35	3022.5	2653.0	1691.9	1829.5	599.7	1321.4	3019.4	20.8	0.02434	2.6	18.7
0.40	2568.6	2325.1	2299.2	1408.3	1739.7	442.6	3239.2	29.6	0.02901	16.0	26.1
0.45	1921.4	1758.0	1218.3	1330.7	773.4	862.8	1957.3	21.7	0.01822	27.1	10.4
0.50	2785.1	2430.2	1987.5	1040.2	770.4	108.4	4382.8	75.3	0.05807	132.3	47.6
0.55	2323.1	2001.1	2160.8	1123.4	1048.3	595.2	2709.9	8.4	0.02686	7.5	19.1
0.60	2837.1	1383.7	1367.5	955.1	691.1	992.8	2136.2	14.6	0.02198	12.1	25.6
0.65	3387.0	2232.5	1684.9	1009.8	1333.6	902.7	2932.6	17.3	0.02477	0.9	15.2
0.70	2094.5	2150.9	1919.4	900.1	770.4	375.7	2781.9	11.3	0.03551	42.0	27.3
	2607.6	2071.3	1718.8	1182.7	981.1	732.0	2676.9	7.1	0.02562	2.5	3.9

Table 4. Virtual experimental results on reconstruction of the dependence between the matrix permeability k_2 and stresses.

1	2	3	4	5	6	7	8	9	10	11	12
P_i MPa	σ_n, MPa						K_2 mD	θ_2 %	α_2 MPa^{-1}	θ_α %	ν_{2i} %
	0	**1**	**2**	**3**	**4**	**5**					
0.20	124.9	119.9	115.1	107.4	102.5	97.0	125.9	0.7	0.00515	3.0	0.7
0.25	123.1	120.8	113.2	106.1	103.2	97.3	124.6	0.4	0.00489	2.2	1.1
0.30	124.8	117.7	113.7	107.2	104.0	98.0	124.3	0.6	0.00469	6.2	0.7
0.35	123.6	119.3	114.8	108.4	103.6	99.2	124.5	0.4	0.00452	9.5	0.5
0.40	124.3	118.9	112.1	108.1	101.0	99.1	124.1	0.8	0.00473	5.3	0.9
0.45	125.0	118.9	112.8	107.1	101.8	96.6	125.0	0.0	0.00516	3.2	0.1
0.50	124.8	119.0	112.2	108.8	101.8	98.0	124.7	0.2	0.00489	2.2	0.6
0.55	123.6	117.7	114.3	107.6	101.7	97.3	124.1	0.7	0.00484	3.2	0.7
0.60	124.4	119.9	112.6	105.9	102.7	96.9	124.9	0.1	0.00508	1.6	0.7
0.65	126.2	119.2	112.5	107.5	101.9	96.2	125.9	0.7	0.00534	6.9	0.3
0.70	123.9	118.2	114.1	109.2	102.0	97.6	124.5	0.4	0.00480	4.1	0.7
	124.4	119.0	113.4	107.6	102.4	97.6	124.8	0.2	0.00492	1.6	0.2

At each P_i, by the least square method, we find the values of K_m (columns 8, Tables 3 and 4) and α_m (columns 10) in the empirical relations

$$k_m(i,n) \cong K_m \exp(-\alpha_m \sigma),$$ (18)

as well as the relative errors $\theta_m = |1 - K_m/K_m^*|$ and $\theta_\alpha = |1 - \alpha_m/\alpha_m^*|$ (columns 9 and 11). Columns 12 (Tables 4 and 5) present the variation factors

$$\nu_{mi} = \sqrt{N \sum_{n=1}^{N} \left[k_m(i,n) - K_m \exp(-\alpha_m \sigma_n)\right]^2} \Big/ \sum_{n=1}^{N} k_m(i,n)$$

characterizing the integral approximation error (18), $N=6$ is the number of stress levels in the virtual model experimentation. It is seen that, despite a small error of the input data, at some P_i the function $k_1(\sigma)$ (line 3 in Fig. 4) is determined at the considerable error as compared with reference function (line 1). After averaging the inversion data of $k_m(i,n)$

obtained at all values of the input pressure P_i (last lines in Tables 4 and 5), the variation factor is never higher than 5% at any random values $\omega_s(i,n)$ in (14) (line 2 in Fig. 4).
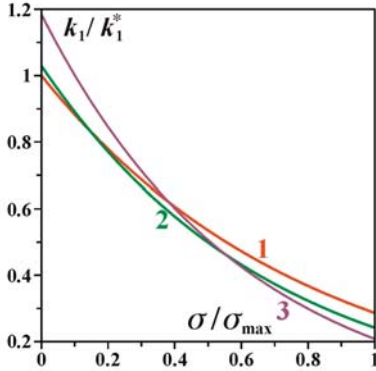

Fig. 4. Stress-dependent permeability k_1 of fissures.

5 Conclusion

The authors have developed and theoretically, based on virtual experimentation, substantiated the method that makes it possible to quantitatively estimate the mass exchange factor β and to establish the empirical dependence of permeability on stresses in fractured porous reservoir rocks. The interpretation of the synthetic input data is implemented within the model of continuum with dual porosity, for which the exact solution of the problem on steady-state fluid flow is obtained. The analytical expressions are derived for determining permeabilities of fissures and matrix as well as the coefficient β by flow rates measured in three different measurement designs. As yet the value of β has been determined only in an operating well by the pressure build-up curve while the proposed procedure allows such estimating in laboratory using standard equipment.

References

1. L. P. Dake, *The Practice of Reservoir Engineering* (Elsevier, 2001)
2. P. R. Robinson, C. S. Hsu, *Introduction to Petroleum Technology. Handbook of Petroleum Technology* (Springer, 2017)
3. S. N. Zakirov, *Gas, Gas-Condensate and Oil-Gas-Condensate Reservoir Engineering.* (Struna, 1998)
4. V. L. Karnaukhov, E. M. Piyankova, *Modern Methods of Drill-Hole Hydrodynamic Survey* (Infra-Inzheneriya, 2010)
5. V. N. Dakhnov, *Interpretation of Geophysical Logging Data* (Nedra, 1982)
6. T. Djebbar, E. C. Donaldson, *Petrophysics. Theory and Practice of Measuring Reservoir Rock and Fluid Transport Properties* (Elsevier, 2016)
7. T. V. Dorofeeva, *Petroleum reservoirs of Bazhenov formation* (*Western Siberia*). Nedra, (1983).
8. G. I. Barenblatt, Yu. P. Zheltov, I. N. Kochina, Prikl. Mat. Mekh. **24**, 5: 852–864 (1960)
9. R. Hill, J. Mech. Phys.Solids. **11**, 5: 357–372 (1963)

10. O. Coussy, *Mechanics and Physics of Porous Solids* (John Wiley & Son Ltd, 2010)

11. Y.-S. Wu, *Multiphase fluid flow in porous and fractured reservoirs* (Elsevier, 2016)

12. S. Salimzadeh, N. Khalili, Int. J. Geomech. **16**, 3 (2015)

13. J. Rutqvist, Y.-S. Wu, C.-F.Tsang, G. Bodvarsson, Int. J. of Rock Mech. Min. Sci. **39**: 429–442 (2002)

14. J. Douglas jr., T. Arbogast, *Dynamics of Fluids in Hierarchical Porous Media*, J. H. Cushman, ed. 177–221 (Academic Press, 1990)

15. R.-S. Nie, Y.-F. Meng,·Y.-Lu. Jia et al., Transport in Porous Media. **92**, 1: 213–235 (2012)

16. M. Presho, S. Wo, V. Ginting, J. of Petroleum Sci. Eng. **77**, 3–4: 326–337 (2011)

17. L. A. Nazarova, L. A. Nazarov, J. of Min. Sci. **52**, 3: 424–431 (2016)

18. P. Thararoopa, Z. T. Karpyn, T. Ertekinc, J. of Natural Gas Sci. Eng. **8**: 121–131 (2012)

19. D. N. Espinoza, M. Vandamme, P. Dangla, J.-M. Pereira, S. Vidal-Gilbert, J. Geophys. Res. Solid Earth. **118**: 6113–6123 (2013)

20. L. A. Nazarova, L. A. Nazarov, M. Vandamme, J.-M. Pereira, J. Applied and Industrial Mathematics. **11**, 2: 236–243 (2017).

21. L. A. Nazarova, L. A. Nazarov, M. Vandamme, J.-M. Pereira, Doklady Phys. **62**, 6: 323–327 (2017)

22. L. J. Hosking, H. R. Thomas, M. Sedighi, Canadian Geotech. J. **55**, 6: 839–851 (2018)

23. T. Babadagli, X. Ren, K. Develi, Int. J. Multiph. Flow. **68**: 40–58 (2015)

24. B. Jones, L. Brouwers, M. Dippenaar, Hydrogeol. J. **26**: 945–961 (2017)

25. T. van Golf-Racht, *Fundamentals of Fractured Reservoir Engineering* (Elsevier, 1982)

26. F. Kuchuk, J. of Petroleum Technology. **47**, 1: 36–41 (1995)

27. D. Bourdet, *Handbook of Petroleum Exploration and Production. V.3. Well Test Analysis* (Elsevier, 2002)

28. X. Yang, T. J. Lu, T. Kim, Phys Lett. A. **378**: 2308–2311 (2014)

29. L. J. Durlofsky, Water Resources Res. **27**, 5: 699–708 (1991)

30. Z. Q. Huang, J. Yao, Y. J. Li et al., Commun. Comput. Phys. **9**: 180–204 (2011)

31. A. Teimoori, Z. Chen, S. S. Rahman, T. Tran, Petroleum Sci. Tech. **23**, 5-6: 693–709 (2005)

32. R. M. Holt, SPE Formation Evaluation. 5: 444–448 (1990)

33. R. Heller, J. Vermylen, M. Zoback, AAPG Bull. **98**, 5 : 975–995 (2014)

34. R. Roi, X. Paredes, R. Holtzman, Earth and Planetary Sci.Lett. **493**: 198–207 (2018)

35. S. Chabezloo, J. Sulem, S. Guedon, F. Martineau, Int. J. Rock Mech. Min. Sci. **46**, 2: 297–306 (2009)

36. Y. Geng, D. Tang, H. Xu et al., Fuel. **202**: 12–22 (2017)

37. D. W. Rhett, L. W. Teufel, SPE Paper 24756. SPE Annual Tech. Conf. Exhibition. (1992).

38. M. S. Randall, M. Conway, G. Salter, S. Miller, AAPG Search and Discovery Article N 9012.2011 (2010).

39. H. Daigle, E. Rasromani, K. E. Gray, J. Petr. Sci. Eng. **157**: 302–311 (2017)

40. L. A. Nazarova, L. A. Nazarov, M. I. Epov, I. N. Eltsov, J. Min. Sci. **49**, 5: 704–714 (2013)

41. I. N. Yeltsov, G. V. Nesterova, A. Y. Sobolev, M. I. Epov, L. A. Nazarova, L. A. Nazarov, Russian Geol. Geoph. **55**, 5–6: 775–783 (2014)

42. M. D. Zoback, A. Nur, AAPG Bull. **95**: 154–158 (1975)

43. J. Ma, J. Rock Mech. Geotech. Eng. **7**, 3: 351–357 (2015)

44. P. Pollard, AIME. **216**: 38-43 (1959)

45. RF State Standard 26450.2-85. *Rocks. Method for determination of absolute gas permeability coefficient by stationary and non-stationary filtration* (1985)

46. www.flowcontrolnetwork.com